Available online at www.qu.edu.iq/journalcm
JOURNAL OF AL-QADISIYAH FOR COMPUTER SCIENCE AND MATHEMATICS
ISSN:2521-3504(online) ISSN:2074-0204(print)

Effect of local thermal non-equilibrium on the onset of convection in an anisotropic bidispersive porous layer

Israa M. Mankhi [(a)], ***Shatha A. Haddad*** [(b)]

a *Department of Mathematics, College of Sciences, University of Basrah, Basrah, Iraq .Email: israa1761986@gmail.com*

b Department of Mathematics, College of Sciences, University of Basrah, Basrah, Iraq .Email: shathahaddad@hotmail.com

ARTICLE INFO

Article history:
Received: 18 /04/2021
Rrevised form: 15 /05/2021
Accepted : 21 /06/2021
Available online: 21 /06/2021

Keywords:Bidispersive porous medium, Local thermal non-equilibrium, Linear instability, anisotropic permeability, Darcy model.

ABSTRACT

The onset of thermal convection of a fluid saturated anisotropic bidisperse porous medium under the condition of local thermal non-equilibrium is investigated. We have studied the case of flow in the macropores and micropores when the porous materials are of Darcy type. The temperatures in the macropores and micropores are allowed to be different. We concentrate our attention on the state of a permeability tensor is transversely isotropic with the isotropy axis in the vertical direction of gravity and the permeability ratios of vertical to horizontal are different in the macropores and micropores . The effect of various parameters on the stationary convection is discussed. In particular the effects of macro permeabilities, the micro permeabilities, the measure between the permeability in the macro phase and micro phase , and various interaction parameters on the stationary convection are studied. The numerical results are presented for free-free boundary conditions.

MSC. 41A25; 41A35; 41A36

DOI : https://doi.org/10.29304/jqcm.2021.13.2.813

1. Introduction

Thermal convection in a bidispersive porous medium is one of much current interest due to its practical applications in various fields, such as in heat pipes technologies, catalytic chemistry, methane recovery from coal deposits, and thermal insulation see e.g., Szczygieł [1], Lin et al. [2], Shi and Durucan [3], and Straughan [4]. However, the effects of anisotropy in permeability on thermal convection in porous media are receiving atopic a particular interest.

There are many applications of bidispersive anisotropic porous medium. Such as to carbon sequestration, landslides, nuclear waste treatment, stockpiling of coal, hydraulic fracturing for natural gas see e.g. Straughan [5, 6], Carneiro [7], Hill and Morad [8], Borja et al. [9], Montrasio et al. [10], Di et al. [11], Kim and Moridis [12], Hooman

∗Corresponding author: Israa M. Mankhi.

Email addresses: *israa1761986@gmail.com*.

Communicated by: *Dr.Rana Jumaa Surayh aljanabi*.

and Maas [13], Hooman et al. [14] and Said et al. [15]. It is worth mentioning that the effect of anisotrop on thermal convection in a bidispersive porous medium has been the subject of much recent research. See for example Straughan [16], who investigated the onset of convection for thermal convection in a bidispersive porous medium, when the horizontal permeability are the same in the macopores and the micopores The same author in Straughan [16] performed the linear and nonlinear stability methods when the permeability ratios in the macropores and the micropores are taken to be different. Saleh and Haddad [17] presented an analysis of linear and nonlinear stability to study the anisotropy parameter with soret coefficient effects on the onset of thermal convection in double porosity media. Saleh [18] also considered the Brinkman model to investigate thermosolutal convection in a bidispersive porous medium with anisotropic permeability effect. Recently, Capone et al. [19] performed linear and nonlinear stability analysis for the problem of thermal convection in an inisotropic and rotating bidisperse porous medium. They found that the linear theory is capturing the physics of the onset of thermal convection. It is important to note that the above mentioned studies have been conducted assuming local thermal equilibrium between the fluid and solid matrix phases. However, for a single porosity body, the effect of anisotropy with local thermal non-equilibrium on thermal instability has been studied intensely by many researchers. For instance, Govender and Vadasz [20] considered the effect of the thermal anisotropy and mechanical anisotropy on the stability, where both the fluid and solid phase are in thermal non-equilibrium. Later, Malashetty et al. [21] analyse the linear instability theory to investigate the effect both of the thermal non-equilibrium and permeability anisotropy on the onset of convection. Shivakumara et al. [22] also deal with the effect of local thermal non-equilibrium and the mechanical and thermal anisotropy parameters on the stability of the system. The same authors, in Shivakumara et al. [23] also deal with the effect of anisotropy combined with the local thermal non-equilibrium effect on thermal convection in a rotating fluid saturated porous medium. Kulkarni Sridhar [24] performed linear instability for a rotating anisotropic porous medium in the presence of thermal non-equilibrium. We take this opportunity to point out that the effects of various parameters such as Peclet number, magnetic parameter,Grashof number, radiation parameter, rotating, Hall parameter, Hartman number, Reynolds number and artificial compressibility parameter, are investigated in general by many authors cf. Mohammed et al. [25], Al-Aridhee et al. [26], Hasen and Abdulhadi [27], Ali and Abdulhadi [28], Jassim and Al-Muslimawi [29].

In this paper, we restrict our attention to the case of the macro permeability tensor and the micro permeability tensor are horizontally isotropic the case in which the permeability varies in the vertical direction cf. Tyvand [30] and Straughan [31]. The main reason for the interest in horizontally isotropic permeability is that most materials possess this property such as soils or rocks cf. Karmakar and Raja Sekhar [32], Ayan et al. [33] and Widarsono et al. [34].
Our main interest is to investigate the combined effect of anisotropy parameter and thermal non-equilibrium on the onset of convection .The values of critical Rayleigh number of linear instability theory are obtained numerically by using Matlab routines.

In the following section the basic equations and the non-dimensionalised perturbation equations are presented. Linear stability is the subject of sections 3. In section 4, the numerical results are reported.

2. Governing Equations

We consider an incompressible fluid saturated a horizontal bidispersive porous layer $\{(x, y) \in \mathbb{R}^2 \times (0 < z < d)\}$ with the temperatures $T^s = T^f = T^p = T_L$ at $z = 0$ and $T^s = T^f = T^p = T_U$ at $z = d$, where T_L, T_U are constants with $T_L > T_U$. Furthermore, we suppose that the solid phase and fluid phase of the medium are in local thermal non-equilibrium and the permeabilities of the saturated bidisperse porous medium are anisotropic. Therefore, the permeability tensors may be written as

$$m_{ij}^f = \begin{bmatrix} \mu/K_I^f & 0 & 0 \\ 0 & \mu/K_I^f & 0 \\ 0 & 0 & \mu/K_\perp^f \end{bmatrix}, \qquad m_{ij}^p = \begin{bmatrix} \mu/K_I^p & 0 & 0 \\ 0 & \mu/K_I^p & 0 \\ 0 & 0 & \mu/K_\perp^p \end{bmatrix},$$

where K_I^f is the horizontal component of macro permeability, $K_\perp^f$ is the vertical component of the macro permeability, K_I^p is the horizontal component of the micro permeability , and $K_\perp^p$ is the vertical component of micro permeability. Where K_I^f, $K_\perp^f$, K_I^p, $K_\perp^f$ are constants.

The basic equation for thermal convection in an anisotropic bidispersive porous medium of Darcy type with U_i^f and U_i^p being the pore-averaged velocities in the macropores and micropores, p^f and p^p are the pressures in the macropores and micropores, μ is the dynamic viscosity, g_i is the gravity vector, ρ_o is reference density, ζ is an interaction coefficient and α the thermal expansion coefficient of the fluid may be written as, cf. Straughan [35] and Saleh and Haddad [17]

$$
\begin{aligned}
&-m_{ij}^f U_i^f - \zeta\,(U_i^f - U_i^p) - p_{,i}^f - \frac{g_i\rho_o\alpha\phi}{D}T^f - \frac{g_i\rho_o\alpha(1-\phi)\varepsilon}{D}T^p = 0,\\
&U_{i,i}^f = 0,\\
&-m_{ij}^p U_i^p - \zeta\,(U_i^p - U_i^f) - p_{,i}^p - \frac{g_i\rho_o\alpha\phi}{D}T^f - \frac{g_i\rho_o\alpha(1-\phi)\varepsilon}{D}T^p = 0,\\
&U_{i,i}^p = 0,\\
&\varepsilon_1(\rho c)_s T_{,t}^s = \varepsilon_1\kappa_s\Delta T^s + s_1(T^f - T^s) + s_2(T^p - T^s),\\
&\phi(\rho c)_f T_{,t}^f + \phi(\rho c)_f V_i^f T_{,i}^f = \phi\kappa_f\Delta T^f + h(T^p - T^f) + s_1(T^s - T^f),\\
&\varepsilon_2(\rho c)_p T_{,t}^p + \varepsilon_2(\rho c)_p V_i^p\, T_{,i}^p = \varepsilon_2\kappa_p\Delta T^p + h\big(T^f - T^p\big) + s_1(T^s - T^p).
\end{aligned}
\tag{1}
$$

where $D = \phi + (1-\phi)\varepsilon$, T^s, T^f and T^p, respectivety, are reference values of temperature in the macropores, micropores, and solid skeleton. ϕ is the microporosity, ε is the microporosity. Standard indicial notation is employed in (1) and throughout. We let $U_i^f = \phi V_i^f$ and $U_i^p = (1-\phi)\varepsilon V_i^p$ are the fluid velocities in the macropores and micropores, V_i^f and V_i^p are the pore average velocities in the macropores and micropores.

where $\varepsilon_1 = (1-\varepsilon)(1-\phi)$, $\varepsilon_2 = (1-\phi)\varepsilon$. Here $(\rho c)_s$, $(\rho c)_f$, $(\rho c)_p$ are the products of the density and the specific heat at constant pressure in the solid in the fluid in the macropores, and in the fluid in the micropores, respectively. The terms κ_s, κ_f and κ_p are thermal conductivities in the solid, and in the fluid in the macropores and micropores, respectively. We denote by s, f and p the solid, the macropores, and the micropores The terms h, s_1 and s_2 are interaction coefficients, and we have here assumed that the interactions are linear in the temperature differences.

The permeability tensors D_{ij}^f and E_{ij}^p are defined as

$$
D_{ij}^f = \begin{bmatrix} 1 & 0 & 0 \\ 0 & 1 & 0 \\ 0 & 0 & h^* \end{bmatrix}, \qquad E_{ij}^p = \begin{bmatrix} 1 & 0 & 0 \\ 0 & 1 & 0 \\ 0 & 0 & k^* \end{bmatrix}
$$

where $h^* = K_l^f/K_\perp^f$ and $k^* = K_l^p/K_\perp^p$ refer to the measure between the permeability in horizontal and vertical directions, respectively, in the macro permeability and the micro permeability, then we may write

$$
m_{ij}^f = \frac{\mu}{K_l^f} D_{ij}^f, \qquad m_{ij}^p = \frac{\mu}{K_l^p} E_{ij}^p.
$$

Suppose that the fluid-saturated bidispersive porous medium satisfies equation (1). The velocity boundary conditions are $U_i^f n_i = 0$, $U_i^p n_i = 0$ at $z = 0, d$ The steady solution in whose stability we are interested has form

$$
\overline{U}_i^f \equiv 0 \quad , \overline{U}_i^p \equiv 0, \qquad \overline{T}^s = \overline{T}^f = \overline{T}^p = -\beta_1 z + T_L = 0
$$

where

$$\beta_1 = \frac{T_L - T_U}{d},$$

To investigate the stability of the steady solution, the perturbation is introduced $(u_i^f, u_i^p, \pi^f, \pi^p, \theta^f, \theta^p, \theta^s)$ in such a way that

$$\begin{aligned} U_i^f &= \bar{U}_i^f + u_i^f, & U_i^p &= \bar{U}_i^p + u_i^p, \\ p^f &= \bar{p}^f + \pi^f, & p^p &= \bar{p}^p + \pi^p, \\ T^s &= \bar{T}^s + \theta^s, \quad T^f = \bar{T}^f + \theta^f, \quad T^p &= \bar{T}^p + \theta^p. \end{aligned}$$

The nonlinear perturbation equations arising from equation (1) are

$$\begin{aligned} &-m_{ij}^f u_i^f - \zeta(u_i^f - u_i^p) - \pi_{,i}^f - \frac{g\, k_i \rho_0 \alpha \phi}{D}\theta^f - \frac{g\, k_i \rho_0 \alpha(1-\phi)\varepsilon}{D}\theta^p = 0, \\ &u_{i,i}^f = 0, \\ &-m_{ij}^p u_i^p - \zeta(u_i^p - u_i^f) - \pi_{,i}^p - \frac{g\, k_i \rho_0 \alpha \phi}{D}\theta^f - \frac{g\, k_i \rho_0 \alpha(1-\phi)\varepsilon}{D}\theta^p = 0, \\ &u_{i,i}^p = 0, \\ &\varepsilon_1 (\rho c)_s \theta_{,t}^s = \varepsilon_1 \kappa_s \Delta\theta^s + s_1(\theta^f - \theta^s) + s_2(\theta^p - \theta^s), \\ &\phi(\rho c)_f \theta_{,t}^f + (\rho c)_f u_i^f \theta_{,i}^f - (\rho c)_f \beta\, w^f = \phi\kappa_f \Delta\theta^f + h\,(\theta^p - \theta^f) + s_1(\theta^s - \theta^f), \\ &\varepsilon_2 (\rho c)_p \theta_{,t}^p + (\rho c)_p u_i^p \theta_{,i}^p - (\rho c)_p \beta\, w^p = \varepsilon_2 \kappa_p \Delta\theta^p + h\,(\theta^f - \theta^p) + s_2(\theta^s - \theta^p). \end{aligned} \tag{2}$$

where $w^f = u_3^f$ and $w^p = u_3^p$, while $k_i = (0,0,1)$. The nonlinear perturbation equations are non- dimensionalisation with the scallings

$$\tau = \frac{d^2(\rho c)_f}{k_f}, \quad p = d\zeta U, \quad U = \frac{k_f}{(\rho c)_f d}, \quad \chi = \frac{\zeta K_I^f}{\mu}, \quad \widehat{w} = \frac{K_I^f}{K_I^p}, \quad T^{\#} = U\sqrt{\frac{\beta\mu(\rho c)_f d^2}{\rho_o \alpha g K_I^f \kappa_m}},$$

where $\widehat{w}$ the measure between the permeability in the macro phase and micro phase.

The Rayleigh number $R_a = R^2$ is given by

$$R^2 = \frac{(\rho c)_f d^2 \beta g \rho_o \alpha K_I^f}{\mu\phi\kappa_f}.$$

Other non-dimensional variables are required and these are given by

$$L_s = \frac{(\rho c)_s}{(\rho c)_f}, \quad L_P = \frac{(\rho c)_p}{(\rho c)_f}, \quad \xi_s = L_s\frac{\varepsilon_1}{\phi}, \quad \xi_p = L_P\frac{\varepsilon_2}{\phi} \quad S_1 = \frac{s_1 d^2}{\phi k_f}, \quad S_2 = \frac{s_2 d^2}{\phi k_f},$$

$$H = \frac{h d^2}{\phi k_f}, \quad \Gamma_s = \frac{\varepsilon_1 k_s}{\phi k_f}, \quad \Gamma_p = \frac{\varepsilon_2 k_p}{\phi k_f}.$$

The nonlinear non-dimensional perturbation equations are

$$
\begin{aligned}
&-\mathrm{D}_{ij}^{f}\mathrm{u}_{i}^{f}-\chi(\mathrm{u}_{i}^{f}-\mathrm{u}_{i}^{p})-\pi_{,i}^{f}+\mathrm{R}\frac{\phi\mathrm{k}_{i}}{\mathrm{D}}\theta^{f}+\mathrm{R}\frac{(1-\phi)\varepsilon\mathrm{k}_{i}}{\mathrm{D}}\theta^{P},\\
&\mathrm{u}_{i,i}^{f}=0,\\
&-\widehat{w}\mathrm{E}_{ij}^{p}\mathrm{u}_{i}^{p}-\chi(\mathrm{u}_{i}^{p}-\mathrm{u}_{i}^{f})-\pi_{i}^{p}+\mathrm{R}\frac{\phi\mathrm{k}_{i}}{\mathrm{D}}\theta^{f}+\mathrm{R}\frac{(1-\phi)\varepsilon\mathrm{k}_{i}}{\mathrm{D}}\theta^{P},\\
&\mathrm{u}_{i,i}^{p}=0,\\
&\xi_{s}\theta_{,t}^{s}=\Gamma_{s}\Delta\theta^{s}+\mathrm{S}_{1}(\theta^{f}-\theta^{s})+\mathrm{S}_{2}(\theta^{p}-\theta^{s}),\\
&\theta_{,t}^{p}+\frac{1}{\phi}\mathrm{u}_{i}^{f}\theta_{,i}^{f}=\mathrm{Rw}^{f}+\Delta\theta^{f}+\mathrm{H}(\theta^{p}-\theta^{f})+\mathrm{S}_{1}(\theta^{s}-\theta^{f}),\\
&\xi_{p}\theta_{,t}^{p}+\frac{\mathrm{L}_{p}}{\phi}\mathrm{u}_{i}^{p}\theta_{,i}^{p}=\mathrm{RL}_{p}\mathrm{w}^{p}+\mathrm{L}_{p}\Delta\theta^{p}+\mathrm{H}(\theta^{f}-\theta^{p})+\mathrm{S}_{2}(\theta^{s}-\theta^{p}).
\end{aligned}
\tag{3}
$$

The corresponding boundary conditions for the problem are

$$
\mathrm{w}^{f}=\mathrm{u}_{3}^{f}=0,\quad \mathrm{w}^{p}=\mathrm{u}_{3}^{p}=0,\quad \theta^{f}=0,\quad \theta^{p}=0,\quad \theta^{s}=0,\quad \text{at } \mathrm{z}=0,1 \tag{4}
$$

3. Linear Instability

In this section, in order to study the linear instability of the system (3) we neglect nonlinear term. We then assume

$$
\begin{aligned}
u_{i}^{f}&=u_{i}^{f}(x)e^{\sigma t}, \qquad u_{i}^{p}=u_{i}^{p}(x)\,e^{\sigma t},\\
\pi^{f}&=\pi^{f}(x)\,e^{\sigma t}, \qquad \pi^{p}=\pi^{p}(x)\,e^{\sigma t},\\
\theta^{f}&=\theta^{f}(x)\,e^{\sigma t}, \quad \theta^{p}=\theta^{p}(x)\,e^{\sigma t}, \quad \theta^{s}=\theta^{s}(x)\,e^{\sigma t}.
\end{aligned}
$$

where σ is a general eigenvalue to obtain. Then π^{f} and π^{p} are eliminated by taking the curl curl of equations $(3)_1$ and $(3)_2$, and using the third component yields

$$
\begin{aligned}
&(h^{*}\Delta^{*}w^{f}+w_{,zz}^{f})+\chi(\Delta w^{f}-\Delta w^{p})-R\frac{\phi}{D}\Delta^{*}\theta^{f}-R\frac{(1-\phi)\varepsilon}{D}\Delta^{*}\theta^{p}=0,\\
&u_{i,i}^{f}=0,\\
&\widehat{w}(k^{*}\Delta^{*}w^{p}+w_{,zz}^{p})+\chi(\Delta w^{p}-\Delta w^{f})-R\frac{\phi}{D}\Delta^{*}\theta^{f}-R\frac{(1-\phi)\varepsilon}{D}\Delta^{*}\theta^{p}=0,\\
&u_{i,i}^{p}=0,\\
&\sigma\xi_{s}\theta_{,t}^{s}=\Gamma_{s}\Delta\theta^{s}+S_{1}(\theta^{f}-\theta^{s})+S_{2}(\theta^{p}-\theta^{s}),\\
&\sigma\theta_{,t}^{f}=Rw^{f}+\Delta\theta^{f}+H(\theta^{p}-\theta^{f})+S_{1}(\theta^{s}-\theta^{f}),\\
&\sigma\xi_{p}\theta_{,t}^{p}=RL_{p}w^{p}+\Gamma_{p}\Delta\theta^{p}+H(\theta^{f}-\theta^{p})+S_{2}(\theta^{s}-\theta^{p}),
\end{aligned}
\tag{5}
$$

where $\Delta^* = \partial^2/\partial x^2 + \partial^2/\partial y^2$, is the horizontal Laplacian. Then we employ the normal modes to solve (5), cf. Chandrasekhar [36], with the representations for $w^f, w^p, \theta^f, \theta^p$ and θ^s in the form of

$$\theta^f = \Theta^f(z)f(x,y), \qquad \theta^p = \Theta^p(z)f(x,y), \qquad \theta^s = \Theta^s(z)f(x,y),$$

$$w^f = W^f(z)f(x,y), \qquad w^p = W^p(z)f(x,y)$$

where f is the horizontal plan form, which satisfies $\Delta^* f = -a^2 f$, a is a wavenumber. Then, allow $W^f, W^p, \Theta^f, \Theta^p$ and Θ^s to be composed of $\sin n\pi z$ for $n \in N$ which satisfies the boundary conditions equation (4). The system (5) may be written in the form

$$\begin{bmatrix} -(\Lambda_{h^*} + \chi\Lambda) & \chi\Lambda & R\frac{\phi}{D}a^2 & R\frac{(1-\phi)\varepsilon}{D}a^2 & 0 \\ \chi\Lambda & -(\widehat{w}\Lambda_{k^*} + \chi\Lambda) & R\frac{\phi}{D}a^2 & R\frac{(1-\phi)\varepsilon}{D}a^2 & 0 \\ 0 & 0 & -S_1 & -S_2 & \xi_S\sigma + \Gamma_S\Lambda + S_1 + S_2 \\ -R & 0 & \sigma + \Lambda + H + S_1 & -H & -S_1 \\ 0 & -L_pR & -H & \xi_p\sigma + \Gamma_p\Lambda + H + S_2 & -S_2 \end{bmatrix} \begin{bmatrix} W^f \\ W^p \\ \Theta^f \\ \Theta^p \\ \Theta^s \end{bmatrix} = \begin{bmatrix} 0 \\ 0 \\ 0 \\ 0 \\ 0 \end{bmatrix}, \qquad (6)$$

where $\Lambda = n^2\pi^2 + a^2$, $\Lambda_h^* = n^2\pi^2 + h^*a^2$ and $\Lambda_k^* = n^2\pi^2 + k^*a^2$. Then, one may consider the following two cases.

3.1 Stationary convection

Substituting ($\sigma = 0$) in equation (6) and setting the determinant of the matrix to zero, one may show

$$\mathrm{R}_{\mathrm{sta}}^2 = \frac{\mathrm{D}\Lambda[\mathrm{P}_0\mathrm{A}_1 + \mathrm{P}_0\mathrm{A}_2]}{\mathrm{a}^2[\phi(\mathrm{P}_2\mathrm{B}_3 - \mathrm{P}_1\mathrm{B}_1) + (1-\phi)\varepsilon(\mathrm{P}_1\mathrm{B}_2 - \mathrm{P}_2\mathrm{B}_4)]}. \qquad (7)$$

With the coefficients $P_0, P_1, P_2, , A_1, A_2, B_1, B_2, B_3,$ and B_4 given by

$P_0 = \chi^2\Lambda^2 - ((\Lambda_{h^*} + \chi\Lambda)(\widehat{w}\Lambda_{k^*} + \chi\Lambda))$

$P_1 = 2\chi\Lambda + \Lambda_{h^*}$

$P_2 = 2\chi\Lambda + \widehat{w}\Lambda_{k^*}$

$A_1 = 2S_1S_2H + S_2^2(\Lambda + H + S_1) + H^2(\Gamma_s\Lambda + S_1 + S_2),$

$A_2 = (\Gamma_p\Lambda + H + S_2)(S_1^2 - (\Lambda + H + S_1)(\Gamma_s\Lambda + S_1 + S_2)),$

$B_1 = S_1S_2L_p + L_pH(\Gamma_s\Lambda + S_1 + S_2),$

$B_2 = S_1^2L_p - L_p(\Lambda + H + S_1)(\Gamma_s\Lambda + S_1 + S_2),$

$B_3 = (S_2^2 - (\Gamma_s\Lambda + S_1 + S_2)(\Gamma_p\Lambda + H + S_2),$

$B_4 = S_1S_2 + H(\Gamma_s\Lambda + S_1 + S_2).$

3.2 Oscillatory convection

In this section the instability is considered by oscillatory convection. Put $\sigma = i\sigma_I$ into equation (6), where $\sigma_I \in \mathbb{R}$. After solving the determinant equation, one can obtain

$$R_{os}^2 = \frac{D\Lambda[P_0(h_1 + h_2 + h_3)]}{-a^2[P_1L_p\xi_S(1-\phi)\varepsilon + P_2\phi\xi_S\xi_p]}. \qquad (8)$$

where h_1, h_2 and h_3 are the coefficients as given

$$h_1 = \xi_s(\Gamma_p \Lambda + H + S_2),$$

$$h_2 = \xi_p(\Gamma_s \Lambda + S_1 + S_2),$$

$$h_3 = \xi_s \xi_p(\Lambda + H + S_1).$$

Numerical method are used to find the stationary and oscillatory convection threshold, respectively, by minimizing R^2 in equations (8) and (9) over a^2. The numerical results are presented in the next section.

4. Numerical results

In the present analysis, we study numerically system (2) to compute the critical Rayleigh number for stationary convection equation(7) and oscillatory convection equation (8), for free-free boundary condition, by using Matlab routines. All numerical results are obtained by varying the number of $h^*, k^*, \widehat{w}$ and for different values of the porosity modified interaction coefficients S_1 and S_2. The parameters $\Gamma_s, \Gamma_p, L_p, \varepsilon, \phi$ and H for all cases we have studied are fixed at 0.1, 0.1, 15, 0.00001, 0.9999 and 0.00001, respectively. The effect of both anisotropy and thermal non-equilibrium on the onset of convection is investigated. It is important to note that the Critical Rayleigh number for oscillatory convection in the presence of anisotropy permeability, in all cases, the instability manifests as stationary convection.

In Table (1), and in Figures(1) and (2) taking $\widehat{w} = 0.1,0.5,1,2$ and 10 with fixed values $S_1 = 0.01$ and $S_2 = 0.1$, and allowing h^* and k^* to vary between 0.1 and 10. Here we find that as h^* increases with k^* fixed, the critical Rayleigh number increases and the critical wavenumber decreases. For example, for fixed values of k^*, $\widehat{w} = 10$ and $h^* = 0.1$ see from Table (1) that the critical Rayleigh number $R_a = 46.0297$ and the critical wavenumber is $a_{sta} = 5.134487$, whereas when $h^* = 10$ for the same parameters $k^* = 1$ and $\widehat{w} = 10$, the critical Rayleigh number is $R_a = 56.130845$ and the critical wavenumber is $a_{sta} = 4.6605867$. Therefore, the effect of increasing the horizontal macro permeability to the vertical macro permeability h^* is seen to increas the critical Rayleigh number and thus the convection occures more easily and the layer more stable as shown in Figures(1). Furthermore, the critical wavenumber decreases which corresponds to the wider convection cells. Figures (2), shows when the horizontal micro permeability to the vertical micro permeability k^* increases as well as $\widehat{w}$ increases, the critical Rayleigh number ,R_a, increases. This indicates that the system became more stable. It is also interesting to note that when $h^* = k^*$ the R_a increases and a_{sta} decreases as $\widehat{w}$ increases. Note that the critical Rayleigh number became significantly higher, $R_a = 89.75967$, at $h^* = k^* = 10$ and the critical wave number became smaller, $a_{sta} = 1.798598$, which leads to stabilizer the system and the convection cells became wider as seen in Table (1).

In Figures (3) and (4) and Table (2), we show how critical Rayleigh number, R_a, respectively, varies with the porosity modified interaction coefficients S_1 and S_2 for various value of $k^* = h^*$. We observe that as h^* and k^* increases from $k^* = h^* = 1$ to $k^* = h^* = 10$ and for fixed value of S_1 and the critical Rayleigh number , R_a, increases. This means when the horizontal macro permeability to the vertical macro permeability h^* and the horizontal micro permeability to the vertical micro permeability k^* increases, the stability becomes more pronounce. For example, for $k^* = h^* = 1$ and fixed values of $S_1 = 0.1$ and $S_2 = 2$ we see from Tabel (2) that the critical Rayleigh number is $R_a = 347.9993$ and the critical wavenumber is $a_{sta} = 5.55105$, whereas when $k^* = h^* = 10$, $S_1 = 0.1$ and $S_2 = 2$ the critical Rayleigh number is $R_a = 1363.6499$ and the critical wavenumber is $a_{sta} = 1.421105$.

Figures (3) and (4) and Table (3) indicate that in interesting the porosity modified interaction coefficients S_2 for a fixed value of h^* and k^* has the effect of making the system more stable wheres an opposite behavior is noticed when S_1 increases, for fixed values of h^* and k^*

In Figures (5) and (6), the critical Ra Rayleigh yleigh number , R_a, variation as S_1 and S_2 varies, respectively, in the range 0.1-1 for $k^* = 10$ and various values of h^*. It is observe that keeping the micro permeability k^* the same, increasing the horizontal micro permeability to the vertical micro permeability strongly increases the critical Rayleigh number as S_2 increases as shown in Figure (5). The opposite behaviour is seen when S_1 increases as shown in Figure (6). This indicates that increasing h^* with S_1 is to hasten the onset of convection. For example, from Table (2), taking $S_2 = 0.1$ and $k^* = 10$, it is found that the value of $R_a = 57.2762$, $a_{sta} = 2.5259$ when $h^* = 1$ and $S_1 = 1$, whereas when $h^* = 10$ and $S_1 = 2$ the value of $R_a = 48.0992$, $a_{sta} = 2.7559$. In addition, for $S_1 = 0.1$ and $K^* = 10$,

we have $R_a = 322.1577$, $a_{sta} = 2.4911$ when $h^* = 1$ and $S_2 = 1$. From Figures (7) and (8) and from Table (2) we show the behaviour of R_a versus S_1 and S_2, respectively, for a fixed value of $h^* = 10$ and $k^* = 1$ increasing to $k^* = 10$. We note that as the horizontal micro permeability to the vertical micro permeability k^* increases, the critical Rayleigh number , R_a, increases. This indicates that keeping the macro permeability h^* the same, increasing k^* delay the onset of convection. The effect of increasing S_1 for a fixed value of S_2, and increasing S_2 for a fixed value of S_1, on the onset of convection is qualitatively similar to that show, respectively, in Figures (5) and (6).

In Figures (9) and (10), we fixed $h^* = 10$ and $k^* = 0.1$ and show the critical Rayleigh number , R_a, varation as S_1 and S_2 varies, for various interaction coffeccient $\chi = 0.1$ to $\chi = 0.9$. The same trend as already reported, in Figures (7) and (8), is again found that with fixed values of S_2 and χ, once S_1 increased will advance the onset of convection. However, when S_2 increased with fixed values of S_1, the critical Rayleigh number , R_a, increases and it becomes more difficult for convection to occur.

Table (3), presents details of R_a and a_{sta} varation as S_1 and S_2 increases and χ taking the values 0.1 and 0.9 when $S_1 = S_2 = 0.1$ increasing to $S_1 = S_2 = 10$, the critical Rayleigh number , R_a, increases and the critical wavenumber decreases but relatively slowly as χ increase from 0.1 to 0.9. Thus, the interaction coefficient χ and the porosity modified interaction coefficient S_1 and S_2 play a major role on the stability characteristics of the system.

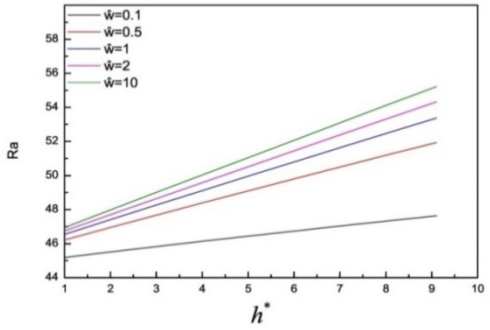

Fig. 1- Critical values of ,R_a , aginst h^* with $\hat{w} = 0.1$, increasing to $\hat{w} = 10$

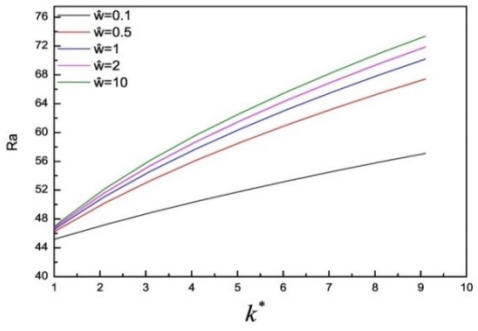

Fig. 2- Critical values of ,R_a aginst k^* with $\hat{w} = 0.1$, increasing to $\hat{w} = 10$

Table 1 – Critical Rayleigh numbers and wave number, aginst h^*, $k^*$and $\hat{w}$, for $\varepsilon = 0.00001$, $\phi = 0.9999$, $\chi = 0.1$, $\Gamma_s = 0.1$, $\Gamma_p = 0.1$, $L_p = 15$, $S_1 = 0.01$, $S_2 = 0.1$, $H = 0.00001$.

h^*	k^*	$\hat{w}$	Ra	a_{sta}
0.1	1	0.1	44.8954	5.0061
2	1	0.1	45.5109	4.9727
1	0.1	0.1	43.4108	5.5998
1	2	0.1	47.0077	4.5163
1	1	0.1	45.1902	4.9898
0.1	1	0.5	45.5642	5.0814
2	1	0.5	46.9500	5.0081
1	0.1	0.5	42.3791	6.8396
1	2	0.5	49.8623	4.1667
1	1	0.5	46.2243	5.0458
0.1	1	10	46.0297	5.1345
10	1	10	56.1308	4.6606
1	0.1	10	41.8479	8.5853
1	10	10	75.4490	2.0384
10	10	10	89.7597	1.7986

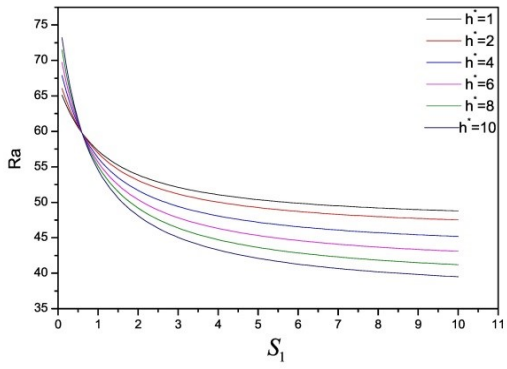

Fig. 3- Critical values of ,R_a , aginst S_1 , $h^* = 1$, increasing to $h^* = 10$

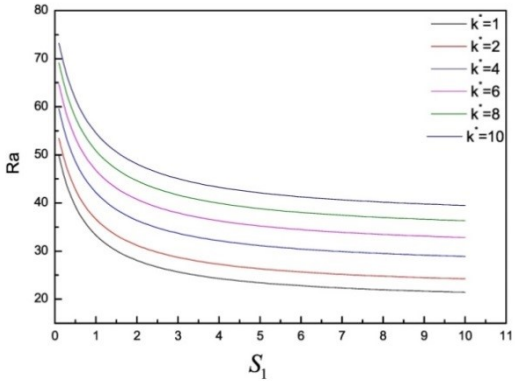

Fig. 4- Critical values of ,R_a , aginst S_1 , $k^* = 1$, increasing to $k^* = 10$

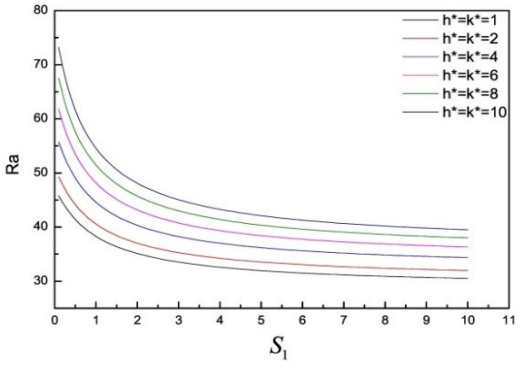

Fig. 5- Critical values of ,R_a , aginst S_1 , $h^* = k^* = 1$, ncreasing to $h^* = k^* = 10$

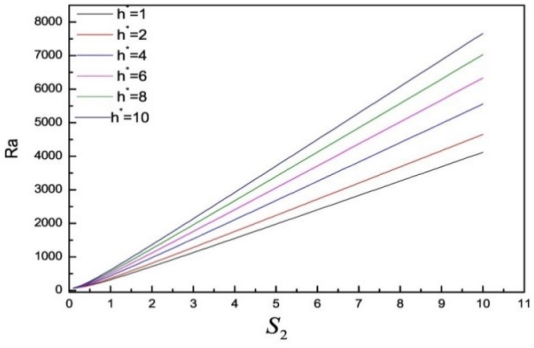

Fig. 6- Critical values of ,R_a , aginst S_2 , $h^* = 1$, increasing to $h^* = 10$

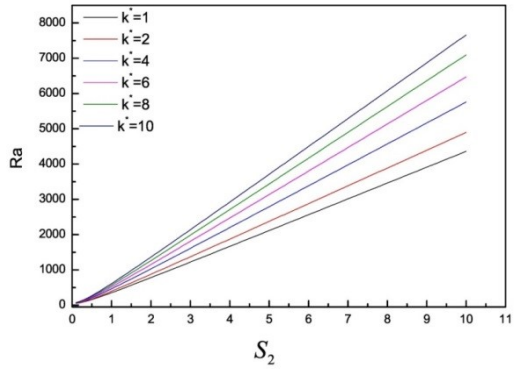

Fig. 7- Critical values of ,R_a , aginst S_2 , $k^* = 1$, increasing to $k^* = 10$

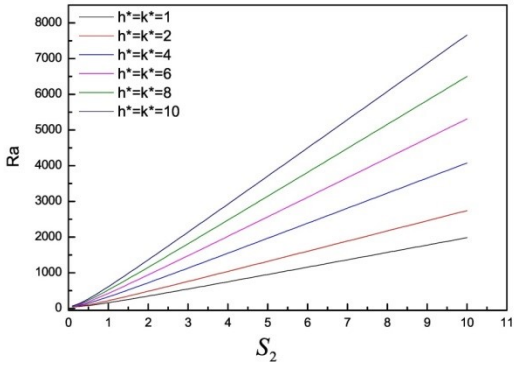

Fig. 8- Critical values of ,R_a , aginst S_2 , $h^* = k^* = 1$, increasing to $h^* = k^* = 10$

Table 2 - Critical Rayleigh numbers and wave number, aginst h^* k^* S_1, S_2, for $\varepsilon = 0.00001$, $\phi = 0.9999$, $\chi = 1$, $\Gamma_s = 0.1$, $\Gamma_p = 0.1$, $L_p = 15$, $\hat{w} = 2$, $H = 0.00001$.

h^*	k^*	S_1	S_2	Ra	a
1	1	1	0.1	38.2805	4.7950
1	1	2	0.1	35.1126	4.8010
1	1	0.1	1	161.6976	5.7807
1	1	0.1	2	347.9993	5.5510
10	10	1	0.1	54.5551	2.6132
10	10	2	0.1	48.0992	2.7560
10	10	0.1	1	612.5364	1.4963
10	10	0.1	2	1363.6499	1.4211
1	10	1	0.1	57.2762	2.5259
1	10	10	0.1	48.7789	2.5675
10	1	1	0.1	33.2996	5.2134
10	1	10	0.1	21.4513	6.2194
1	10	0.1	1	322.1577	2.4911
1	10	0.1	10	4118.2939	2.2338
10	1	0.1	1	353.6250	3.4807
10	1	0.1	10	4361.9037	3.1430

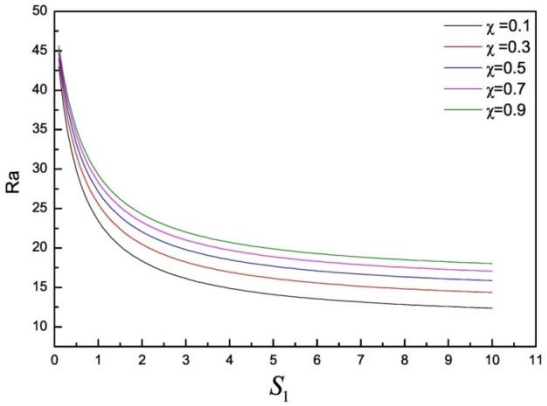

Fig. 9- Critical values of ,R_a ,

$\chi = 0.1$ increasing to $\chi = 0.9$

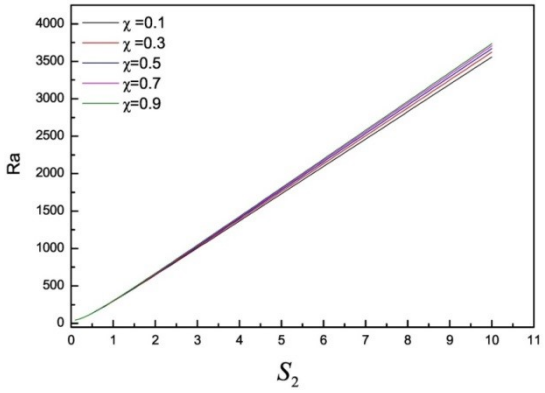

Fig. 10- Critical values of ,R_a ,

$\chi = 0.1$ increasing to $\chi = 0.9$

Table 3 - Critical Rayleigh numbers and wave number, aginst S_1 S_2, χ, for $\varepsilon = 0.00001$, $\phi = 0.9999$, $\Gamma_s = 0.1$, $\Gamma_p = 0.1$, $L_p = 15$, $\hat{w} = 2$, $h^* = 10$, $k^* = 0.1$, $H = 0.00001$.

S_1	S_2	χ	Ra	a
0.1	0.1	0.1	43.0294	7.7427
10	0.1	0.1	12.3711	11.0881
0.1	10	0.1	3558.1226	5.6885
10	10	0.1	91.7649	10.4634
0.1	0.1	0.9	45.6435	6.0105
10	0.1	0.9	18.0277	7.7772
0.1	10	0.9	3734.3842	4.2977
10	10	0.9	124.1974	7.4850

5. Conclusion

The stability of the Darcy flow in a bidispersive porous medium is analysed, under the assumption that the fluid phase and solid phase of the porous medium are in local thermal non-equilibrium. For all situations, the convection instability threshold for stationary is show to be below the oscillatory convection.

Our analysis emphasied that the effect of macro permeabilities h^* and the micro permeabilities k^* when $h^* = k^*$ as $\widehat{w}$ increase, for fixed values of S_1 and S_2, is to stabilize the system. It is also very noticeable that the convection sets in earlier for small value of $k^* < 1$ and large value of $\widehat{w}$. However, as k^* increase, for a fixed value of h^* and $\widehat{w}$, R_{sta} increases. The same qualitative behavior is found when $\widehat{w}$ and k^* are fixed and h^* increase. This indicates that the effect of the measure between the permeability in the macro phase and micro phase $\widehat{w}$, the horizontal macro permeability to the vertical macro permeability h^*, and the horizontal micro permeability to the vertical micro permeability k^* is to enhance the stability of the system. It may be argued from the results that the onset of thermal convection is significantly influenced by the porosity modified interaction cofficients $S_1$and S_1. Increasing the value of S_2, for fixed values of h^* and k^*, and for fixed value of interaction coefficient is to increase, the critical Rayleigh number. The effects of increasing S_1 were seen to advance the onset of convection.

References

[1] J. Szczygieł, Enhancement of reforming efficiency by optimising the porous structure of reforming catalyst: Theoretical considerations, Fuel 85 (2006) 1579–1590.
[2] F.-C. Lin, B.-H. Liu, C.-C. Juan and Y.-M. Chen, Effect of pore size distribution in bidisperse wick on heat transfer in a loop heat pipe, Heat and mass transfer 47 (2011) 933–940.
[3] J.-Q. Shi and S. Durucan, Gas storage and flow in coalbed reservoirs: implementation of a bidisperse pore model for gas diffusion in coal matrix, SPE Reservoir Evaluation & Engineering 8 (2005) 169–175.
[4] B. Straughan, Convection with local thermal non-equilibrium and microfluidic effects, vol. 32. Springer, 2015.
[5] B. Straughan, Mathematical aspects of multi-porosity continua. Springer, 2017.
[6] B. Straughan, Convection with local thermal non-equilibrium and microfluidic effects, vol. 32. Springer, 2015.
[7] J. F. Carneiro, Numerical simulations on the influence of matrix diffusion to carbon sequestration in double porosity fissured aquifers, International Journal of Greenhouse Gas Control 3 (2009) 431–443.
[8] A. A. Hill and M. Morad, Convective stability of carbon sequestration in anisotropic porous media, Proceedings of the Royal Society A: Mathematical, Physical and Engineering Sciences 470 (2014) 20140373.
[9] R. I. Borja, X. Liu and J. A. White, Multiphysics hillslope processes triggering landslides, Acta Geotechnica 7 (2012) 261–269.
[10] L. Montrasio, R. Valentino and G. L. Losi, Rainfall infiltration in a shallow soil: a numerical simulation of the double-porosity effect, Electron. J. Geotechnol. Eng 16 (2011) 1387–1403.
[11] A. S. di Santolo and A. Evangelista, Calibration of a rheological model for debris flow hazard mitigation in the campania region, in Landslides and Engineered Slopes. From the Past to the Future, Two Volumes+ CD-ROM, pp. 935–942. CRC Press, 2008.
[12] J. Kim and G. J. Moridis, Numerical analysis of fracture propagation during hydraulic fracturing operations in shale gas systems, International Journal of Rock Mechanics and Mining Sciences 76 (2015) 127–137.
[13] K. Hooman and U. Maas, Theoretical analysis of coal stockpile self-heating, Fire safety journal 67 (2014) 107–112.
[14] K. Hooman, E. Sauret and M. Dahari, Theoretical modelling of momentum transfer function of bi-disperse porous media, Applied Thermal Engineering 75 (2015) 867–870.
[15] B. Said, A. Grandjean, Y. Barré, F. Tancret, F. Fajula and A. Galarneau, Lta zeolite monoliths with hierarchical trimodal porosity as highly efficient microreactors for strontium capture in continuous flow, Microporous and Mesoporous Materials 232 (2016) 39–52.
[16] B. Straughan, Horizontally isotropic double porosity convection, Proceedings of the Royal Society A 475 (2019) 20180672.
[17] S. H. Saleh and S. A. Haddad, Effect of anisotropic permeability on double-diffusive bidisperse porous medium, Heat Transfer 49 (2020) 1825–1841.
[18] S. H. Saleh, Stability analyses of double diffusion convection in a bidisperse porous media, 2020.
[19] F. Capone, R. De Luca and M. Gentile, Thermal convection in rotating anisotropic bidispersive porous layers, Mechanics Research Communications 110 (2020) 103601.
[20] S. Govender and P. Vadasz, The effect of mechanical and thermal anisotropy on the stability of gravity driven convection in rotating porous media in the presence of thermal non-equilibrium, Transport in porous media 69 (2007)55–66.
[21] M. Malashetty, I. Shivakumara and S. Kulkarni, The onset of lapwood–brinkman convection using a thermal non-equilibrium model, International journal of heat and mass transfer 48 (2005) 1155–1163.
[22] I. Shivakumara, J. Lee, A. Mamatha and M. Ravisha, Boundary and thermal non-equilibrium effects on convective instability in an anisotropic porous layer, Journal of mechanical science and technology 25 (2011) 911–921.
[23] I. Shivakumara, A. Mamatha and M. Ravisha, Local thermal non-equilibrium effects on thermal convection in a rotating anisotropic porous layer, Applied Mathematics and Computation 259 (2015) 838–857.
[24] S. Kulkarni, Unsteady thermal convection in a rotating anisotropic porous layer using thermal non-equilibrium model, .
[25] H. K. Mohammed, W. S. Khudair, R. J. Mezher and Q. A. Shakir, Influence of magneto hydrodynamics oscillatory flow for carreau fluid through regularly channel with varying temperature, Journal of Al-Qadisiyah for computer science and mathematics 11 (2019) Page–13.
[26] A. A. H. Al-Aridhee and D. G. S. Al-Khafajy, Influence of varying temperature and concentration on mhd peristaltic transport for jeffrey fluid with variable viscosity through porous channel, Journal of Al-Qadisiyah for computer science and mathematics 11 (2019) Page–38.
[27] S. S. Hasen and A. M. Abdulhadi, Influence of a rotating frame on the peristaltic flow of a rabinowitsch fluid model in an inclined channel, Journal of Al-Qadisiyah for computer science and mathematics 12 (2020) Page–21.
[28] H. A. Ali and A. M. Abdulhadi, Analysis of heat transfer on peristaltic transport of powell-eyring fluid in an inclined tapered symmetric channel with hall and ohm's heating influences, Journal of Al-Qadisiyah for computer science and mathematics 10 (2018) Page–26.

[29] B. K. Jassim and A. H. Al-Muslimawi, Numerical analysis of Newtonian flows based on artificial compressibility ac method, Journal of Al-Qadisiyah for computer science and mathematics 9 (2017) 115–128.
[30] P. A. Tyvand and L. Storesletten, Onset of convection in an anisotropic porous medium with oblique principal axes, Journal of fluid mechanics 226 (1991)371–382.
[31] B. Straughan and D. Walker, Anisotropic porous penetrative convection, Proceedings of the Royal Society of London. Series A: Mathematical, Physical and Engineering Sciences 452 (1996) 97–115.
[32] T. Karmakar and G. Raja Sekhar, A note on flow reversal in a wavy channel filled with anisotropic porous material, Proceedings of the Royal Society A: Mathematical, Physical and Engineering Sciences 473 (2017) 20170193.
[33] C. Ayan, N. Colley, G. Cowan, E. Ezekwe, P. Goode, F. Halford et al., Measuring permeability anisotropy: The latest approach, Oilfield Review;(Netherlands) 6 (1994) .
[34] B. Widarsono, I. Jaya, A. Muladi et al., Permeability vertical-to-horizontal anisotropy in indonesian oil and gas reservoirs: a general review, in International Oil Conference and Exhibition in Mexico, Society of Petroleum Engineers, 2006.
[35] B. Straughan, Horizontally isotropic bidispersive thermal convection, Proceedings of the Royal Society A: Mathematical, Physical and Engineering Sciences 474 (2018) 20180018.
[36] S. Chandrasekhar, Hydrodynamic and hydromagnetic stability. Courier Corporation, 2013.